Author/s:
Dumont, C;Czuba, E;Chen, M;Villadangos, JA;Johnston, APR;Mintern, JD

Title:
DNA-based probes for flow cytometry analysis of endocytosis and recycling

Date:
2017-04-01

Citation:
Dumont, C., Czuba, E., Chen, M., Villadangos, J. A., Johnston, A. P. R. & Mintern, J. D. (2017). DNA-based probes for flow cytometry analysis of endocytosis and recycling. Traffic, 18 (4), pp.242-249. https://doi.org/10.1111/tra.12466.

Persistent Link:
https://hdl.handle.net/11343/292422

Original Research Article
TRA.12466
doi: 10.1111/TRA.12466
Society number TRA-15-0467
NIH funded NO
Manuscript received 20 December 2015
Revised and accepted 21 December 2016
Sent to press 21 December 2016
Color figures: Figures 1, 2
Halftone figures: Figures 3, 4, 5, 6
Supplemental figures (legends only to be included in typeset manuscript): 4 figures
Synopsis included YES
Abstract figure included YES
Editorial process file included- **NO**

DNA-based probes for flow cytometry analysis of endocytosis and recycling.

Claire Dumont[1], Ewa Czuba [3], Moore Chen[3], Jose A. Villadangos[1,2], Angus P.R. Johnston[3,4*], Justine D. Mintern[1*]

[1] Department of Biochemistry and Molecular Biology, The University of Melbourne, Bio21 Molecular Science and Biotechnology Institute, 30 Flemington Rd, Parkville, Victoria 3010, Australia

[2] Department of Microbiology and Immunology, Peter Doherty Institute for Infection and Immunity, The University of Melbourne, Parkville, Victoria 3010, Australia

[3] Monash Institute of Pharmaceutical Sciences, 381 Royal Parade, Parkville, VIC 3052, Australia

[4]ARC Centre of Excellence in Convergent Bio-Nano Science and Technology, Monash University, Parkville, Australia

Running Title: DNA-based probes for endocytosis measurements.

Key Words: endocytosis, recycling, transferrin, probes

* These authors have made an equal contribution to this manuscript.

Corresponding Authors: Justine D. Mintern, jmintern@unimelb.edu.au; Angus P.R. Johnston

Angus.Johnston@monash.edu

Synopsis:
We demonstrate the utility of a DNA-based specific hybridization internalization probe (SHIP) assay to examine endocytosis and recycling of ligands that bind to receptor proteins using flow cytometry. We monitored endocytosis of membrane-bound transferrin receptor and its soluble ligand transferrin in cell lines and primary cells. We demonstrate that internalization and recycling of holo-transferrin, and an antibody against the transferrin receptor behave differently. SHIP provides a convenient and high throughput technique for analysis of trafficking of cell surface receptors and ligands.

ABSTRACT
The internalization of proteins plays a key role in cell development, cell signaling and immunity. We have previously developed a specific hybridization internalization probe (SHIP) to quantitate the internalization of proteins and particles into cells. Herein, we extend the utility of SHIP to examine both the endocytosis and recycling of surface receptors using flow cytometry. SHIP was used to monitor endocytosis of membrane-bound transferrin receptor and its soluble ligand transferrin. SHIP enabled measurements of the proportion of surface molecules internalized, the internalization kinetics and the proportion and rate of internalized molecules that recycle to the cell surface with time. Using this method, we have demonstrated the internalization and recycling of holo-transferrin, and an antibody against the transferrin receptor behave differently. This assay therefore highlights the implications of receptor internalization and recycling, where the internalization of the receptor-antibody complex behaves differently to the receptor-ligand complex. In addition, we observe distinct internalization patterns for different subpopulations of primary cells. SHIP provides a convenient and high throughput technique for analysis of trafficking parameters for both cell surface receptors and their ligands.

INTRODUCTION
Understanding the endocytosis of cell surface receptors and/or their ligands is important for many cellular functions including cell signaling, antigen presentation and drug delivery[1-3]. Many assays for measuring endocytosis rely on imaging-based or biochemical assays. Flow cytometry offers the advantage of high throughput analysis, however given that it provides no information regarding the location of the fluorescent signal, flow cytometry assays must be modified to distinguish between surface and internalized molecules. Several flow cytometry-based assays have been designed to measure internalization, however, all of these have shortcomings that limit their usefulness, particularly with primary cells. More traditional methods such as acid wash stripping of surface proteins (for example[4-6]) or treatment with proteases[7] can impact cell viability and vary in their effectiveness (for example[8]). These treatments can also remove other phenotypic markers required to distinguish cell subsets in a mixed population. Biotin pulse-chase assays equate a reduction in surface signal to internalization, but neglect to account for loss of molecules by other means such as fast antibody off-rates or antibody shedding from the cell surface[9-11]. Clever use of molecules labeled with different fluorochromes can provide flow cytometry based measurements of protein internalization and recycling[12], however they do not provide direct measurements of internalized signals as they cannot distinguish between signals elicited from the cell surface and the inside of the cell. In contrast, pH sensitive dyes offer the ability to undertake indirect measurements of internalization, with a gain in fluorescent signal following fluorochrome access to an acidic compartment[13]. Unfortunately, often small increases in signal can limit their applicability and their reliance on endosomal acidification means they are not applicable for cell types that have more pH neutral endosomal compartments[14,15]. Finally, a promising new method that directly measures protein internalization is the use of an anti-flourochrome antibody to quench surface-bound fluorochromes. This approach has been used to measure the internalisation[8,16,17] and recycling[8] of several molecules. While useful, antibody-mediated quenching can vary in its efficiency, with some analyses requiring additional controls to ensure adequate exclusion of surface signals[16]. Potential antibody cross-reactivity is another consideration. Currently, while this approach can be applied for Alexa Fluor-488 and Alexa Fluor-594, attempts to generate similar antibodies for Alexa Fluor -647 and Alexa Fluor 750 dyes have been unsuccessful[17].

We have established an endocytosis assay that overcomes the limitations of other flow cytometry based assays by using a specific hybridization internalization probe (SHIP – Figure 1A)[18]. The SHIP assay comprises of two components: a short fluorophore-labeled single-stranded DNA oligonucleotide probe termed fluorescent internalization probe (FIP); and a complementary DNA strand that is conjugated to a quencher dye (QP_c). FIP can be directly attached to an antibody or to a soluble ligand of interest using copper-free click chemistry. By introducing the QP_c at different time points, the internalization of any molecule of interest can be quantified by flow cytometry. We have previously used the SHIP assay to monitor internalization of nanoparticles[18,19], antibody-dependent phagocytosis[20] and to investigate the internalization of immune cell receptors in the context of antibody-targeted vaccination[21]. Here we describe the capacity of SHIP technology to monitor the endocytosis and recycling of membrane bound receptors and/or soluble ligands by flow cytometry. To do this, we have used SHIP to monitor transferrin and transferrin

receptor (TFR) endocytosis. The transferrin cycle, responsible for cellular iron uptake, is extensively characterized and thus provides an ideal framework to demonstrate the usefulness of the SHIP method[22]. Here, for the first time, we have extended the utility of SHIP to monitor the recycling of internalized molecules back to the cell surface. SHIP is an innovative method that permits rapid and high throughput endocytosis analysis.

RESULTS and DISCUSSION

SHIP analysis of TFR internalization. To establish the robustness of the SHIP assay, we investigated the kinetics of transferrin internalization in C1R B lymphoblastoid cells. The transferrin cycle (reviewed in[22]) involves iron-saturated, holo-transferrin (TF) binding to TFR at the cell surface. Following ligand binding, TFR is internalized by clathrin-mediated endocytosis (CME)[23], and then iron dissociates from TF in the low pH of early endosomes. Following dissociation of iron from the TF, the TFR-TF complex recycles to the cell surface and "empty" apo-TF dissociates from TFR and is lost from the cell. To measure TFR endocytosis, FIP was conjugated to OKT9, a mouse monoclonal IgG1 antibody specific for human TFR[24] (anti-TFR_{FIP}). Surface TFR was labeled by incubating C1R cells with anti-TFR_{FIP} at 4°C for 30 min, and the fluorescence intensity was measured using flow cytometry (mean fluorescence intensity, MFI, 2676). Upon the addition of the QP_c, the fluorescence signal was quenched (MFI 334), confirming that TFR is present on the surface of the cell and the FIP is accessible to QP_c. Cells labeled at 4°C were then incubated at 37°C for 9 minutes, after which they showed a similar level of anti-TFR_{FIP} expression (MFI 2824), however in the presence of QP_c, a significant proportion of the anti-TFR_{FIP} signal remains (MFI 1896) (Figure 2A). Microscopy of anti-TFR_{FIP} labeled cells also illustrated the use of the FIP in distinguishing between populations of TFR at the cell surface and those that had undergo internalization from the plasma membrane (Figure 2B).

The kinetics of TFR internalization was monitored with anti-TFR_{FIP}. Again, TFR on the surface of C1R cells was labeled with anti-TFR_{FIP} at 4°C. Excess anti-TFR_{FIP} was washed away and anti-TFR_{FIP} -labeled cells incubated at 37°C for different lengths of time. Following culture, half of the cells were stained with the QP_c, the other half were left unquenched, and the fluorescence intensity was measured using flow cytometry. To probe the mechanisms of internalization, the cells were also cultured in the presence, or absence of Dyngo 4a, a cell permeable inhibitor of dynamin. Dyngo 4a has been shown to potently inhibit transferrin endocytosis[25], likely by inhibiting the scission of the clathrin coated pit from the cell membrane. A concentration of Dyngo 4a was selected that did not significantly reduce C1R viability based on staining with the viable cell exclusion dye propidium iodide (Supplementary Figure 1). First, the stability of the total anti-TFR_{FIP} signal with time (ie. signals elicited from both inside the cell and the cell surface) relative to the surface anti-TFR_{FIP} signal at time 0 was determined. For the duration of the assay in the absence of Dyngo 4a, the total anti-TFR_{FIP} signal remained similar throughout, suggesting anti-TFR_{FIP} is not significantly lost from cells and remains either at the cell surface or inside the cells. In contrast, Dyngo 4a treatment promoted a loss in the overall anti-TFR_{FIP} signal of approximately 20% indicating that under these conditions a small proportion of anti-TFR_{FIP} is lost from the cell (Figure 3A and B).

Next, we assessed the kinetics of anti-TFR_{FIP} internalization. The percentage of internalization can be calculated via equation 1 below, where Q_n is the geometric mean fluorescent intensity (MFI) at time n after the addition of QP_c, Q_0 is the MFI at time 0 after the addition of QP_c, and F_0 is the MFI at time 0 without the addition of the QP_c.

$$\% \text{ internalised} = \frac{Q_n - Q_0}{F_0 - Q_0} \times 100 \quad (1)$$

In the absence of Dyngo 4a, a high proportion of surface anti-TFR_{FIP} is internalized, with ~90% of total surface anti-TFR_{FIP} internalized after 30 minutes (Figure 3C). Surface turnover of anti-TFR_{FIP} occurred rapidly with the majority (80%) of internalized anti-TFR_{FIP} entering the C1R cells within 9 minutes of culture. After 9 min, the percent of internalized anti-TFR_{FIP} plateaued. This plateau is likely due to either a proportion of the anti-TFR_{FIP} remaining on the surface, bound to TFR that doesn't internalize. This plateau could also be due to anti-TFR_{FIP} recycling back to the surface of the cell, leading to a steady state equilibrium of surface and internalized TFR. As expected, in the presence of Dyngo 4a, the proportion of internalized anti-TFR_{FIP} is significantly reduced, with only 20% of total surface anti-TFR_{FIP} internalized after 30 min under these conditions (Figure 3C and D). The internalization of anti-TFR_{FIP} in the

presence of Dyngo 4a shows a steady increase over the 30 min time course, in contrast to the pseudo 1st order kinetics of the internalization in the absence of Dyngo 4a (Figure 3C and D).

We next determined the kinetics of TFR internalization for primary bone marrow B cells using SHIP. Two major B cell sub-populations are present in the bone marrow and can be distinguished based on their expression of cell surface marker B220. Cells exhibit either a $B220^{high}$ or $B220^{int}$ phenotype, with both populations expressing TFR (Figure 4A). Measurement of TFR internalization was performed with FIP conjugated to TIB-219 an anti-mouse TFR IgG2a monoclonal antibody. For both cell types, the proportion of total surface TFR internalized was approximately ~50%, lower than what we observed for C1R internalization of human TFR. Importantly, SHIP analysis of TFR internalization kinetics revealed that the two populations exhibited distinct kinetics of TFR internalization. $B220^{int}$ B cells exhibited a rate of TFR internalization similar to that observed for human TFR expressed by C1R cells, where internalization was rapid with a plateau at 6 minutes. In contrast, $B220^{high}$ cells displayed a significantly slower rate of TFR internalization with no major plateau (Figure 4B). Therefore, these results demonstrate that SHIP enables a quantitative and informative read out of surface molecule internalization for both cell lines and primary cells.

SHIP analysis of TF internalization. Next, we directly conjugated FIP to holo-TF, for analysis of TF_{FIP} endocytosis. A non saturating concentration of TF_{FIP} was chosen for analysis (Supplementary Figure 2). To ensure that FIP conjugation did not overtly alter TF activity, we compared TF_{FIP} to TF conjugated to the Alexa 647 fluorochrome (TF_{A647}). C1R cells were incubated with TF_{FIP} or TFA_{647} at 4°C, excess TF washed away and cells incubated at 37°C in the presence or absence of Dyngo 4a. Incubation was performed in the presence of 100-fold excess cold TF. Analysis of the total TF_{FIP} or TF_{A647} signal after 30 minutes of incubation showed that in both the absence and presence of Dyngo 4a, a high proportion of TF_{FIP} and TF_{A647} is lost from the cells with time, with Dyngo 4a treatment accelerating this loss (Figure 5A). This loss of signal is likely due to a combination of two factors: dissociation of the TF-TFR complex that forms on the surface and dissociation of apo-TF once it is recycled to the surface of the cell[22]. Quantification of TF_{FIP} internalization, where cells were treated with the QP_c prior to flow cytometry, showed that in the absence of Dyngo 4a, TF_{FIP} is rapidly internalized. After 9 min, the percent internalized reached a maximum of ~60%, and then slowly decreased over the next 20 min to ~45% (Figure 5B). The reduction in percentage TF_{FIP} internalized indicates that TF_{FIP} internalized into the cell is then subsequently recycled to the cell surface and ultimately disassociates from the cell. Treatment of C1R cells with Dyngo 4a elicited a significant reduction in TF_{FIP} internalization, with less than 5% of surface TF_{FIP} being internalized (Figure 5B and C). This is in contrast to the inhibition of anti-TFR_{FIP}, which showed a linear increase in internalized receptor (up to 20% after 30 min). This suggests that while the majority of TF_{FIP} is internalized via a dynamin dependent pathway, a portion of anti-TFR_{FIP} is slowly internalized via a dynamin independent pathway.

In summary, SHIP analysis of TF concurs with its expected pattern of endocytosis[26]. The reduction in both the total and internalized TF_{FIP} signal with time is indicative of apo-TF dissociating from TFR and the cell following intracellular iron delivery and return to the cell surface. The loss in total TF_{FIP} signal elicited in the presence of Dyngo 4a, under conditions where we observe almost no TF_{FIP} internalization, suggests TF_{FIP} dissociates from TFR at pH 7.0. The loss of TF_{FIP} signal from the cell, contrasts with that of anti-TFR_{FIP}, which would not be expected to be lost from the cell if it recycles to the surface. This was confirmed by the SHIP data. Patterns of internalization measured for anti-TFR_{FIP} and TF_{FIP} were similar, although Dyngo 4a had a greater impact on TF_{FIP} internalization, where ~95% of internalization is shut down (Figure 4C), compared to 80% inhibition of anti-TFR_{FIP} internalization (Figure 3C), suggesting that a small proportion of anti-TFR_{FIP} is internalized without binding TF, via a route independent of dynamin.

$$\%\ \text{recycled} = \frac{(Q_{\text{int}6} - F_{\text{int}6}Q_{eff}) - (Q_r - F_rQ_{eff})}{Q_{\text{int}6} - F_{\text{int}6}Q_{eff}} \times 100$$

$$Q_{eff} = \frac{Q_0}{F_0}$$

SHIP analysis of recycling. SHIP provides the ability to monitor the recycling of internalized molecules back to the cell surface without extensive cell manipulation or drug treatment. In this case, internalized FIP-bound molecules returning to the cell surface can be detected by re-exposing cells to the QP_c, which will cause a

reduction in the total signal detected given that recycled molecules are now accessible to quenching. We used SHIP to monitor the recycling of internalized anti-TFR and TF to the cell surface. C1R cells were labeled with anti-TFR_{FIP} or TF_{FIP} at 4°C, after which they were incubated at 37°C for six minutes to allow internalization. At this time point, cells were placed on ice and incubated with QP_c to quench any remaining anti-TFR_{FIP} or TF_{FIP} surface signal. Quenched cells containing internalized anti-TFR_{FIP} (or TF_{FIP}) were washed three times to remove excess QP_c and then returned to culture. If excess QP_c was not removed from the cell suspension, a marked decrease in fluorescent signal was observed over time (Supplementary Figure 3). This suggests that if QP_c remains in solution it can be macropinocytosed by the C1R cells, and when the macropinosomes fuse with the endosomal compartments containing anti-TFR_{FIP} or TF_{FIP}, the QP_c quenches the internalized material.

After increasing lengths of time, half of the cells were incubated with the QP_c, the other half were left unquenched, and the fluorescence intensity was analyzed using flow cytometry (Figure 1B). Recycling was calculated via equation 2 below, where: Q_{int6} is the MFI of the cells after anti-TFR_{FIP} or TF_{FIP} have been allowed to internalize for 6 min, and after addition of QP_c; F_{int6} is the MFI at the same time point, but without the addition of QP_c; Q_r is the MFI after the anti-TFR_{FIP} or TF_{FIP} have been allowed to recycle to the surface and after the second addition of the QP_c; F_r is the MFI at the same time point without the addition of QP_c; and Q_{eff} is the quenching efficiency of QP_c, where Q_0 is the MFI at time 0 after the addition of QP_c, and F_0 is the MFI at time 0 without the addition of the QP_c. The F x Q_{eff} term in the equation corrects for the fluorescence of signal that is lost from the cells when TFR_{FIP} or TF_{FIP} dissociate from the cell surface.

(2)

Measurement of anti-TFR_{FIP} recycling with time revealed no significant recycling occurred over 25 min, with the fluorescent signal remaining constant after the addition of the second QP_c (Figure 6A). However for TF_{FIP}, approximately 60% of the internalized TF_{FIP} was recycled back to the surface of the cell after 25 min (Figure 6A). The total fluorescent signal of the cells decreased with time, indicating that TF_{FIP} is lost from the cells. This is in agreement with the internalization results shown in Figure 5. The addition of the second QP_c did not further decrease the fluorescence of the cells. This indicates that TF_{FIP} recycled to the surface of the cell as apo-transferrin immediately dissociates from the receptor. The difference in recycling behavior suggests anti-TFR_{FIP} is directed to non-recycling endosomes, whereas TF_{FIP} is trafficked to recycling endosomes. This is in accordance with studies that show the redirection of TFR for degradation following binding by OKT9 antibody[27]. This has significant implications for the study of receptor internalization and recycling, as the internalization of the receptor-antibody complex likely behaves differently to the receptor-ligand complex.

Next we examined if the recycling kinetics of TF and anti-TFR could be measured in primary bone marrow B cells. Measuring the recycling kinetics in bone marrow $B220^+$ B cells was not possible, as the signal from the quenched TF_{FIP} and anti-TFR_{FIP} increased following the 37ºC incubation (Supplementary Figure 4). This suggests that the hybridized FIP and QP_C denatured when they were internalized into bone marrow B cells. This phenomena was not observed in the C1R cell line, and indicates that denaturing occurs as a result of the specific endocytic pathway by which bone marrow B cells traffic TF and anti-TFR. The loss of quenching does not affect the ability of FIP to measure internalization in the bone marrow B cells, as QP_C is added on ice and there is no internalization of the quenched surface markers during internalization experiments.

To determine if the recycling assay was applicable to other primary cells, we investigated the recycling kinetics in bone marrow $TER119^+$ $fsc^{int\text{-}high}$ erythroblasts[28]. After 6 minutes, approximately 7% of anti-TFR_{FIP} was internalized, compared to 20% internalized in bone marrow B cells and 65% internalized in C1R cells. Similarly, the internalization kinetics of TF_{FIP} in bone marrow erythroblasts were reduced compared to C1R cells (25% vs 45% internalized respectively). This indicates that the bone marrow erythroblasts exhibit slower trafficking kinetics than bone marrow B cells and C1R cells. The signal from quenched anti-TFR_{FIP} and TF_{FIP} did not increase over the 24 minutes of the recycling assay (Supplementary Figure 4), indicating that hybridized FIP and QP_C does not denature when internalized into bone marrow erythroblasts, thus enabling the recycling kinetics to be determined.

In contrast to the recycling observed in C1R cells, both the anti-TFR_{FIP} and TF_{FIP} were rapidly recycled back to the surface of the cell. 80 % of the internalized anti-TFR_{FIP} and TF_{FIP} were recycled back to the surface of the cell after 12 minutes (Figure 6B). Interestingly, as was observed for recycling in C1R cells, the total fluorescent signal of the cells decreased with time, indicating that both TF_{FIP} and anti-TFR_{FIP} were lost from the cells following recycling to the surface.

In summary, the DNA-based SHIP assay enables high throughput analysis of endocytosis by flow cytometry providing robust measurements of parameters of internalization and recycling. Using this assay we have demonstrated the internalization and recycling behavior of an anti-transferrin antibody, and the transferrin ligand is very different, and behaves differently in different primary cell types. This result supports previous findings[27] that when studying receptor internalization, the antibody can play a role in governing the internalization kinetics and pathway via which the receptor is internalized. Here, we have used a single fluorophore to measure internalization of TFR/TF, however this method is amenable for use with different fluorophores to permit simultaneous analysis of multiple receptors/ligands. In depth understanding of the parameters that govern endocytosis is important if the endocytic behaviour of surface molecules and their ligands are to be manipulated in therapeutic settings.

MATERIALS AND METHODS

Cell Lines

Cells lines used in this study were C1R cells, a human B cell lymphoblast cell line and HeLa cells, a human epithelial cell line. Both cell lines were cultured in DMEM supplemented with glutamine, fetal calf serum and antibiotics.

Bone Marrow Cells

Femurs and tibia were removed from 6-12 week old C57Bl/6 mice and single cell suspensions prepared by passing bone marrow through a 25-gauge needle. B cells and erythroblasts were identified by staining cells with fluorescently conjugated anti-B220 and anti-TER119 (Biolegend), respectively.

Transferrin Receptor Antibody and Transferrin

Purified mouse monoclonal IgG1 anti-human transferrin receptor antibody (clone OKT9)[24] was purchased from WEHI Antibody Facility. Anti-mouse transferrin receptor IgG2a monoclonal antibody (clone TIB-219) was purchased from ATCC and purified by the WEHI Antibody Facility. Experiments investigating transferrin trafficking used human iron saturated holo-transferrin (Sigma-Aldrich T0665).

Fluorescence internalization probe

Generation of FIP probes was performed as previously described[29]. In brief, FIP-azide (5' Cy5-TCAGTTCAGGACCCTCGGCT-N_3 3') and QP_C (5' AGCCGAGGGTCCTGAACTGA- BHQ2 3') were purchased from Integrated DNA Technologies, USA. Proteins were functionalized with a strained cyclooctyne (Click-IT succinimidyl ester (SE) DIBO alkyne (Life Technologies, USA) to enable copper-free click coupling of the FIP-azide to the protein. The proteins were incubated with a 10-fold molar excess of SE DIBO for two hours at 4°C. Functionalized antibodies were purified using a Zeba spin desalting column (Thermo Scientific) and incubated with 2-fold molecular excess of FIP-azide at 4°C overnight. FIP-labeled antibody was purified using a 30K MWCO Amicon filter (MerckMillipore), and the degree of functionalization was measured with a NanoDrop 1000 UV-Vis spectrophotometer. Labeling efficiency was determined as the ratio of Cy5-FIP to antibody where antibody concentration was determined by measurement of absorbance at 280 nm (A280) following subtraction of the A280 signal elicited by the Cy5-FIP (0.55 x absorbance at 649 nm).

Microscopy

Cell membranes were labeled with RFP Cell Light (Life Technologies). Cells were stained for 30 minutes on ice with FIP-Cy5 conjugated monoclonal antibody in complete DMEM. Staining was followed by two washes. FIP-antibody bound cells were incubated in complete DMEM at 37ºC, 10% CO_2 or on ice for 9 minutes followed by addition, or not, of 1 μM Quencher in DMEM media. Cells were fixed with 4% paraformaldehyde and permeabilized with 0.3% Triton X-100. Nuclei were stained with Hoescht. Images were obtained with a LSM710 confocal microsope (Zeiss).

Internalization Assay

SHIP internalization assays were performed by staining cells on ice for 30 minutes with FIP-Cy5 conjugated monoclonal antibody or FIP-Cy5 conjugated ligand. Staining was followed by two washes and incubation of anti-TFR_{FIP} or TF_{FIP} bound cells in complete DMEM at 37ºC, 10% CO_2. Assays were performed in the absence of serum. Where indicated, cells were incubated in the presence of Dyngo4a (Abcam). Cells were

removed at specific time points and placed on ice. After the time course cells were washed. For bone marrow cells, cells were stained with fluorescently conjugated antibodies for the identification of specific cell populations. Staining was performed on ice for 30 minutes. Cells were washed and resuspended in media containing propridium iodide with or without 1 μM QP_C. Cells were analysed using a BD LSRFortessa. Data was analyzed with FlowJo (Tree Star).

Recycling Assay

SHIP recycling assays were performed by staining cells on ice for 30 minutes with FIP-Cy5 conjugated monoclonal antibody or FIP-Cy5 conjugated ligand. Staining was followed by two washes and incubation of FIP-antibody/ligand bound cells in complete DMEM at 37ºC, 10% CO_2 for 6 minutes. After 6 minutes, the cells were placed on ice for 30 minutes and 1 μM of QP_C was added. After 5 minutes, the excess QP_C was removed by washing the cells 3 times in DMEM, and were placed at 37ºC, 10% CO_2. Cells were removed at specific time points and placed on ice. For bone marrow cells, cells were stained with fluorescently conjugated antibodies for the identification of specific cell populations. Staining was performed on ice for 30 minutes. Cells were washed, and resuspended in media containing propidium iodide with or without 1 μM QP_C. Cells were analysed using a BD LSRFortessa. Data was analyzed with FlowJo (Tree Star).

ACKNOWLEDGEMENTS

This research was supported by a National Health and Medical Research Council Project Grant (1062549) the Australian Research Council through the Future Fellowship Scheme (FT110100265 – APRJ) and Centre of Excellence in Convergent Bio-Nano Science and Technology (APRJ). APRJ is also supported through the Monash University Larkin's Fellowship Scheme. All authors declare no conflict of interest.

FIGURE LEGENDS

Figure 1. Schematic Representation of the SHIP Internalization and Recycling Assays. (A) To measure internalization using SHIP, first ligand or antibody labeled with FIP is incubated with the cells at 4ºC. Excess FIP is washed from the sample and the cells are incubated at 37ºC for various periods of time. iii) Before analysis using flow cytometry, the QP_c is added to quench surface fluorescence. The fluorescence intensity of the quenched sample quantifies the relative number of internalized receptors, and by determining the ratio of the quenched fluorescence with the fluorescence intensity before the addition of the QP_c, the percentage of internalized receptor can be determined. (B) i) To measure recycling of molecules, FIP functionalized ligand or antibody is bound to the surface of the cell and allowed to internalize for a fixed period of time (6 min for this TF study). ii) The cells are placed at 4ºC and the surface fluorescence quenched. iii) After excess quencher has been removed, the cells are incubated at 37ºC for various periods of time to allow the recycling of receptors back to the cell surface. iv) Before analysis using flow cytometry, the QP_c is added to quench surface fluorescence. A loss fluorescence intensity indicates the recycling of receptor back to the cell surface.

Figure 2. Parameters of SHIP analysis. (A) C1R cells stained with anti-TFR_{FIP} at 4°C, were exposed (top right panel), or not to QP_c (top left panel). anti-TFR_{FIP} labeled cells were cultured for 9 minutes at 37°C and exposed (bottom right panel) or not to QP_c (bottom left panel). Representative histograms of flow cytometry measurement of TFR internalization. (B) HeLa cells expressing RFP Cell Light plasma membrane (green) stained with anti-TFR_{FIP} (red) at 4°C, were exposed, or not to QP_c. anti-TFR_{FIP} labeled cells were cultured for 9 minutes at 37°C and exposed or not to QP_c. Cells were fixed and nuclei were stained with Hoechst (blue).

Figure 3. SHIP analysis of anti-TFR_{FIP} internalization. (A) C1R cells were labeled with anti-TFR_{FIP} at 4°C. Cells were incubated at 37°C for increasing periods of time in the presence, or absence of 30 μM Dyngo 4a. Flow cytometry was performed on cells without exposing them to QP_c. The total anti-TFR_{FIP} signal was normalized to the zero time point (% anti-TFR_{FIP} (total)) and calculated as the ratio of the geometric mean fluorescence intensity at time X (MFI_X) divided by the MFI at time 0 (MFI_0). Data is mean ± SEM, performed in triplicate and representative of 3 independent experiments. (B) Graph displays pooled data from 2 independent experiments performed in triplicate. Data is mean + SD, analysed by unpaired T test. **** $P < 0.0001$. (C). Internalization kinetics of anti-TFR_{FIP} internalization in the presence (open) and absence (solid) of 30 μM Dyngo 4a. % anti-TFR_{FIP} (internalized) was calculated as outlined in Results. (D) Graph displays pooled data from 3 independent experiments performed in triplicate. Data is mean + SD, analysed by unpaired T test. **** $P < 0.0001$.

Figure 4. SHIP analysis of anti-TFR_{FIP} internalization by primary bone marrow B cells. (A) Bone marrow B cells were isolated and TFR internalization by $B220^{int}$ and $B220^{high}$ cells analyzed by SHIP. Data shows representative flow cytometry dot plot illustrating the gating strategy for B220 B cells and histogram overlays of anti-TFR staining at time 0 minutes in the presence and absence of QP_c. (B) Bone marrow cells were labeled with anti-TFR_{FIP} at 4°C. Cells were incubated at 37°C for increasing periods of time and internalization kinetics analyzed as outlined in Results. Data is mean ± SD, pooled from two independent experiments performed in triplicate. * P < 0.05,** P < 0.001, **** P < 0.0001, two-way ANOVA with Bonferroni's multiple comparison test.

Figure 5. SHIP analysis of TF internalization. (A) C1R cells were labeled with TF_{A647} or TF_{FIP} at 4°C. Cells were incubated at 37°C for 30 minutes (in the presence of unlabelled TF) in the presence, or absence of 30 μM Dyngo 4a (Dyngo). Flow cytometry of TF signals was performed on cells without exposing them to QP_c. The total TF_{FIP} signal was normalized to the zero time point (% TF_{FIP} (total). Data is mean + SD, pooled from 2-3 independent experiments performed in triplicate. **** P < 0.0001, ** P < 001, n.s. = not significant, unpaired T test. (B) Cells were labeled with TF_{FIP} and incubated at 37°C for increasing periods of time. Flow cytometry was performed following incubation with 1 μM QP_c. Data is mean ± SEM, performed in triplicate and represents data from 3 independent experiments. (B) Percentage TF_{FIP} internalization was calculated as outlined in Results. Data is mean ± SEM, performed in triplicate and represents data from 3 independent experiments. C) Graph displays pooled data from 3 independent experiments performed in triplicate. Data is mean + SEM, analysed by unpaired T test. **** P < 0.0001.

Figure 6. Flow cytometry-based analysis of anti-TFR_{FIP} and TF_{FIP} recycling. (A) C1R cells or (B) bone marrow erythroblasts were labeled with anti-TFR_{FIP} or TF_{FIP} at 4°C. After receptor binding, cells were incubated at 37ºC for 6 min, cells were placed on ice and incubated with 1 μM QP_c for 1 min. Excess QP_c was washed away after the 1 min incubation. The cells were then incubated at 37°C for increasing periods of time, and were exposed to 1 μM QP_c before flow analysis. Line graphs display percent of anti-TFR_{FIP} and TF_{FIP} recycled over time and bar graphs display percent of anti-TFR_{FIP} and TF_{FIP} recycled after 24 min. Data is mean ± SD, performed in triplicate and represents pooled data from 2 independent experiments. Data is analysed by unpaired T test. **** P < 0.0001, n.s. not significant.

REFERENCES

1. Conner SD, Schmid SL. Regulated portals of entry into the cell. *Nature.* 2003;422(6927):37-44.
2. Canton I, Battaglia G. Endocytosis at the nanoscale. *Chem Soc Rev.* 2012;41(7):2718-2739.
3. Smith AE, Helenius A. How viruses enter animal cells. *Science.* 2004;304(5668):237-242.
4. Carroll RC, Beattie EC, Xia H, et al. Dynamin-dependent endocytosis of ionotropic glutamate receptors. *Proc Natl Acad Sci U S A.* 1999;96(24):14112-14117.
5. Park M, Penick EC, Edwards JG, Kauer JA, Ehlers MD. Recycling endosomes supply AMPA receptors for LTP. *Science.* 2004;305(5692):1972-1975.
6. Karagiannis SN, Warrack JK, Jennings KH, et al. Endocytosis and recycling of the complex between CD23 and HLA-DR in human B cells. *Immunology.* 2001;103(3):319-331.
7. Maier LA, Xu FJ, Hester S, et al. Requirements for the internalization of a murine monoclonal antibody directed against the HER-2/neu gene product c-erbB-2. *Cancer Res.* 1991;51(19):5361-5369.
8. Austin CD, De Maziere AM, Pisacane PI, et al. Endocytosis and sorting of ErbB2 and the site of action of cancer therapeutics trastuzumab and geldanamycin. *Mol Biol Cell.* 2004;15(12):5268-5282.
9. Shi M, Dennis K, Peschon JJ, Chandrasekaran R, Mikecz K. Antibody-induced shedding of CD44 from adherent cells is linked to the assembly of the cytoskeleton. *J Immunol.* 2001;167(1):123-131.
10. Bazil V, Strominger JL. Metalloprotease and serine protease are involved in cleavage of CD43, CD44, and CD16 from stimulated human granulocytes. Induction of cleavage of L-selectin via CD16. *J Immunol.* 1994;152(3):1314-1322.
11. Arribas J, Coodly L, Vollmer P, Kishimoto TK, Rose-John S, Massague

J. Diverse cell surface protein ectodomains are shed by a system sensitive to metalloprotease inhibitors. *J Biol Chem.* 1996;271(19):11376-11382.
12. Peden AA, Schonteich E, Chun J, Junutula JR, Scheller RH, Prekeris R. The RCP-Rab11 complex regulates endocytic protein sorting. *Mol Biol Cell.* 2004;15(8):3530-3541.
13. Miksa M, Komura H, Wu R, Shah KG, Wang P. A novel method to determine the engulfment of apoptotic cells by macrophages using pHrodo succinimidyl ester. *J Immunol Methods.* 2009;342(1-2):71-77.
14. Savina A, Peres A, Cebrian I, et al. The small GTPase Rac2 controls phagosomal alkalinization and antigen crosspresentation selectively in CD8(+) dendritic cells. *Immunity.* 2009;30(4):544-555.
15. Trombetta ES, Ebersold M, Garrett W, Pypaert M, Mellman I. Activation of lysosomal function during dendritic cell maturation. *Science.* 2003;299(5611):1400-1403.
16. Kozik P, Francis RW, Seaman MN, Robinson MS. A screen for endocytic motifs. *Traffic.* 2010;11(6):843-855.
17. Liao-Chan S, Daine-Matsuoka B, Heald N, et al. Quantitative assessment of antibody internalization with novel monoclonal antibodies against Alexa fluorophores. *PLoS One.* 2015;10(4):e0124708.
18. Liu H, Johnston AP. A programmable sensor to probe the internalization of proteins and nanoparticles in live cells. *Angewandte Chemie.* 2013;52(22):5744-5748.
19. Mann SK, Czuba E, Selby LI, Such GK, Johnston AP. Quantifying Nanoparticle Internalization Using a High Throughput Internalization Assay. *Pharm Res.* 2016;33(10):2421-2432.
20. Ana-Sosa-Batiz F, Johnston AP, Liu H, et al. HIV-specific antibody-dependent phagocytosis matures during HIV infection. *Immunol Cell Biol.* 2014;92(8):679-687.
21. Reuter A, Panozza SE, Macri C, et al. Criteria for dendritic cell receptor selection for efficient antibody-targeted vaccination. *J Immunol.* 2015;194(6):2696-2705.
22. Mayle KM, Le AM, Kamei DT. The intracellular trafficking pathway of transferrin. *Biochim Biophys Acta.* 2012;1820(3):264-281.
23. Pearse BM, Robinson MS. Clathrin, adaptors, and sorting. *Annu Rev Cell Biol.* 1990;6:151-171.
24. Sutherland R, Delia D, Schneider C, Newman R, Kemshead J, Greaves M. Ubiquitous cell-surface glycoprotein on tumor cells is proliferation-associated receptor for transferrin. *Proc Natl Acad Sci U S A.* 1981;78(7):4515-4519.
25. McCluskey A, Daniel JA, Hadzic G, et al. Building a better dynasore: the dyngo compounds potently inhibit dynamin and endocytosis. *Traffic.* 2013;14(12):1272-1289.
26. Rothenberger S, Iacopetta BJ, Kuhn LC. Endocytosis of the transferrin receptor requires the cytoplasmic domain but not its phosphorylation site. *Cell.* 1987;49(3):423-431.
27. Weissman AM, Klausner RD, Rao K, Harford JB. Exposure of K562 cells to anti-receptor monoclonal antibody OKT9 results in rapid redistribution and enhanced degradation of the transferrin receptor. *J Cell Biol.* 1986;102(3):951-958.
28. Koulnis M, Pop R, Porpiglia E, Shearstone JR, Hidalgo D, Socolovsky M. Identification and analysis of mouse erythroid progenitors using the CD71/TER119 flow-cytometric assay. *J Vis Exp.* 2011(54).
29. Liu H, Dumont C, Johnston AP, Mintern JD. Analysis of Intracellular Trafficking of Dendritic Cell Receptors for Antigen Targeting. *Methods Mol Biol.* 2016;1423:199-209.

Figure 1

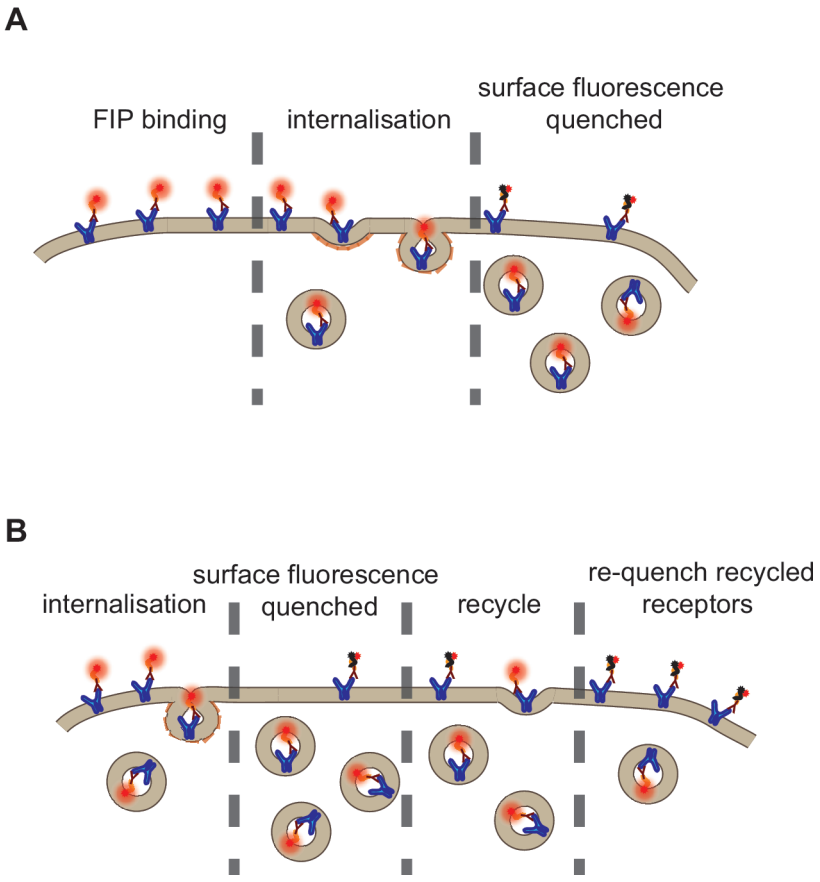

fig1claire_revisednov22.eps

Figure 2

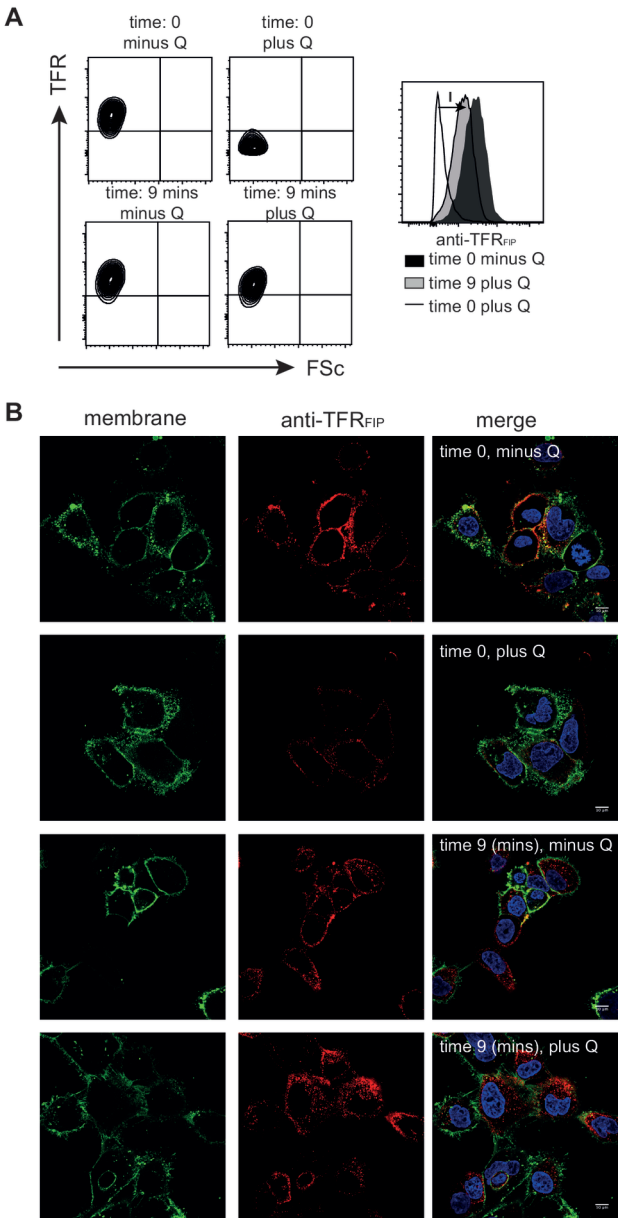

fig2clairepaper_dec20revised.eps

Figure 3

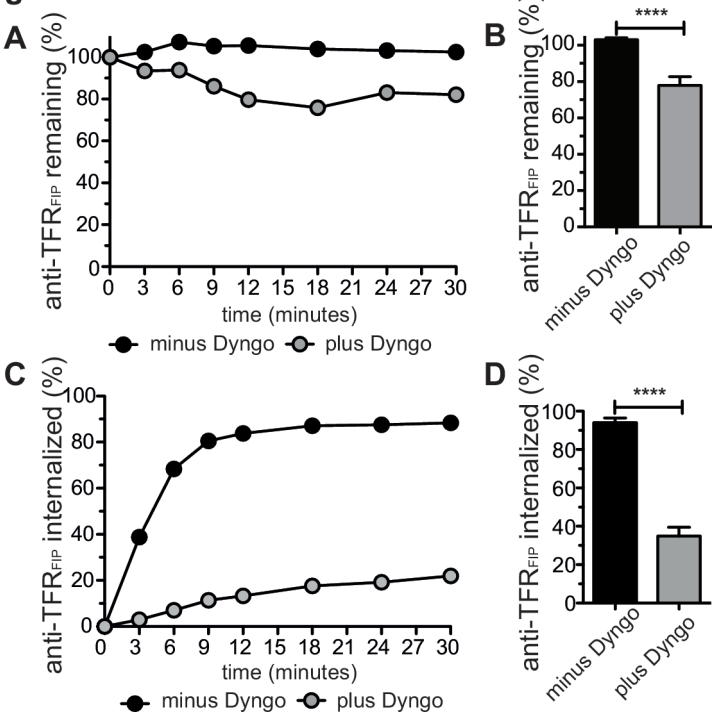

fig3clairepaper_may17.eps

Figure 4

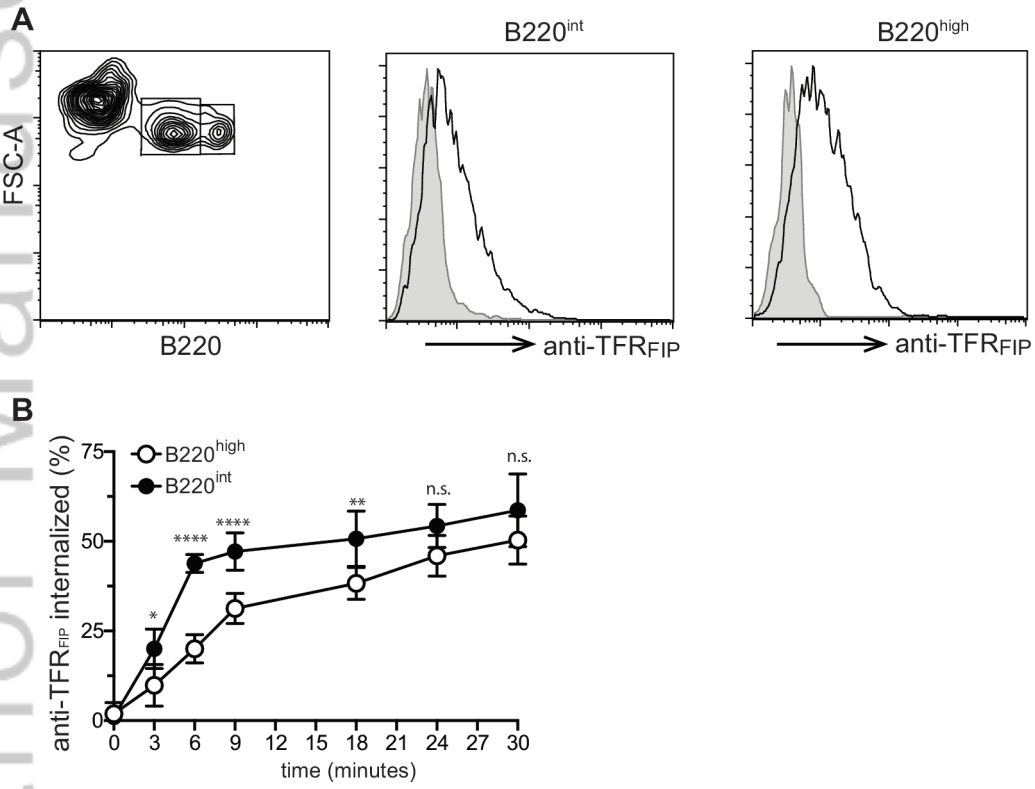

figure4_dec21revised.eps

Figure 6

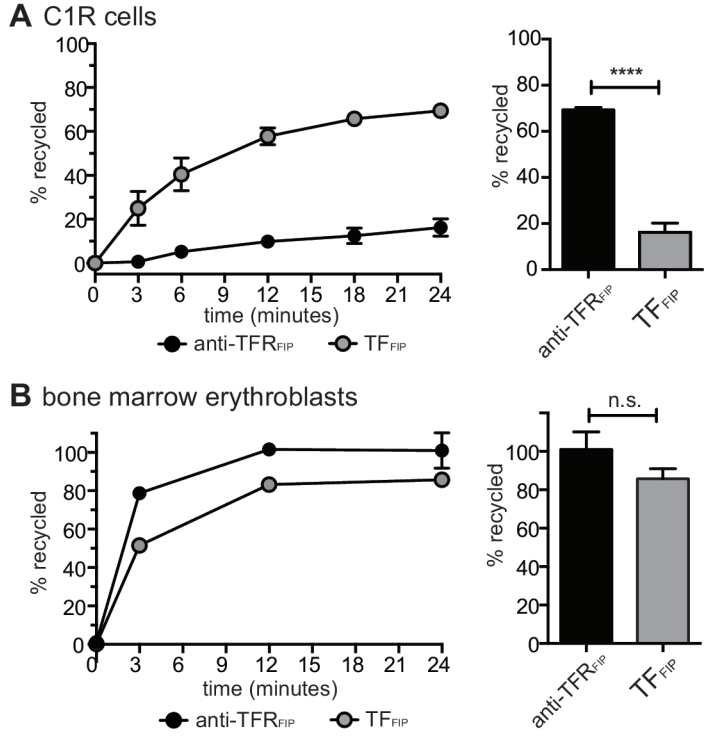

figure6_dec14v2.eps

Figure 5

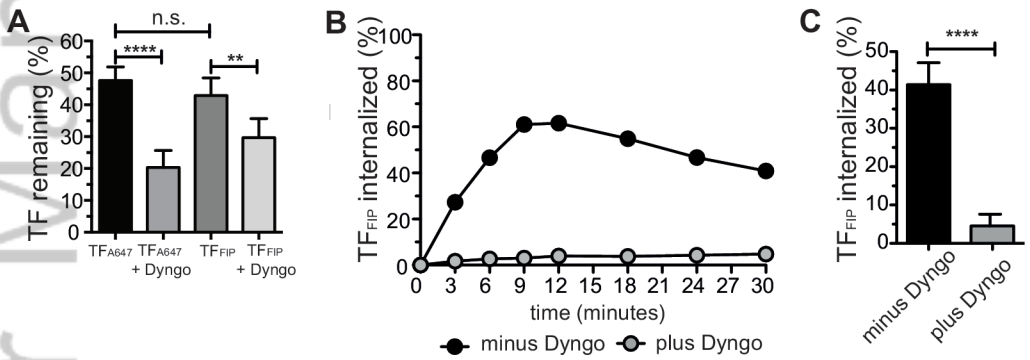

figure5_claire_may17.eps

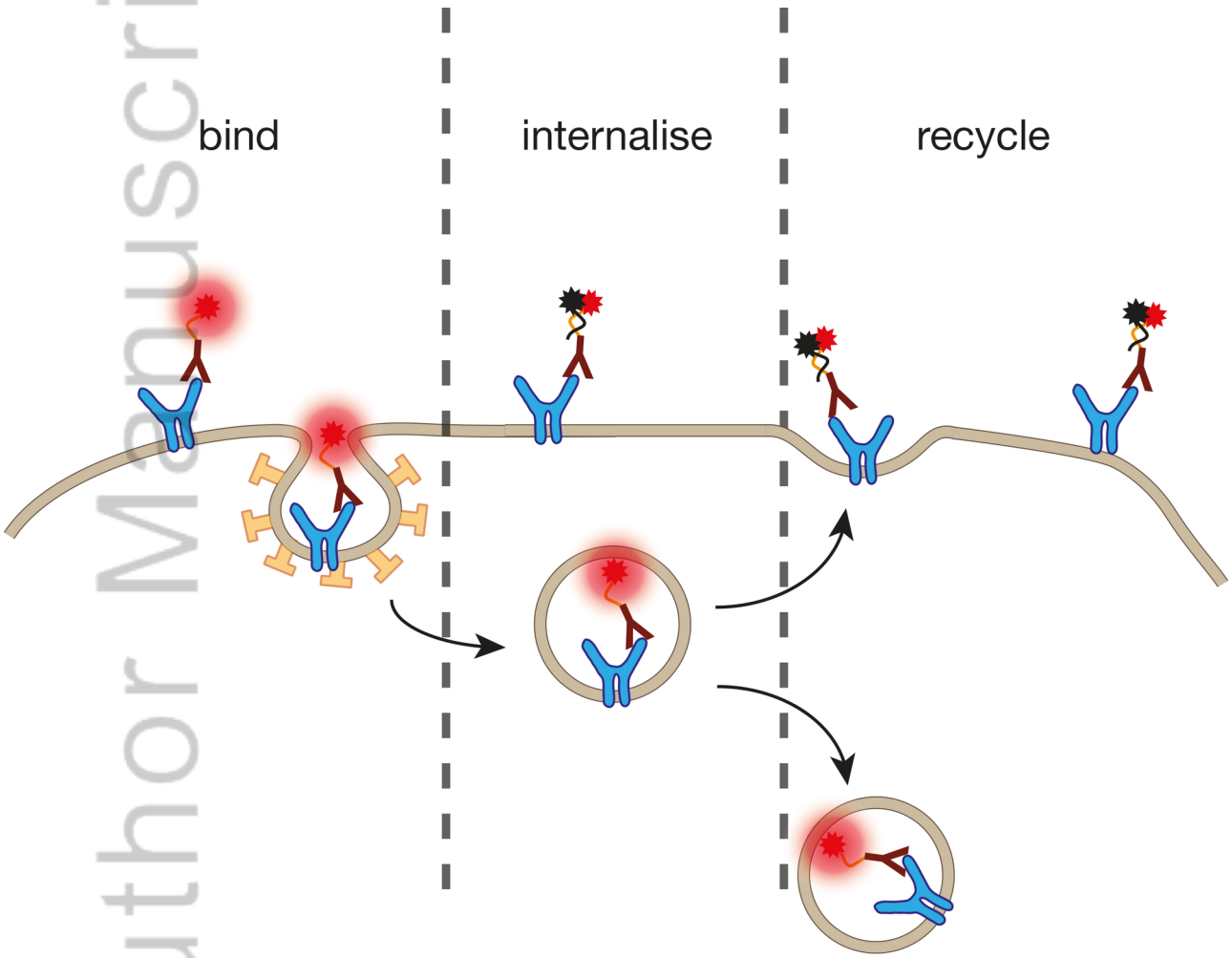

tra_12466_AbstractFigure.tiff

DNA-based probes for flow cytometry analysis of endocytosis and recycling.

Claire Dumont[1], Ewa Czuba [3], Moore Chen[3], Jose A. Villadangos[1,2], Angus P.R. Johnston[3,4*], Justine D. Mintern[1*]

[1] Department of Biochemistry and Molecular Biology, The University of Melbourne, Bio21 Molecular Science and Biotechnology Institute, 30 Flemington Rd, Parkville, Victoria 3010, Australia

[2] Department of Microbiology and Immunology, Peter Doherty Institute for Infection and Immunity, The University of Melbourne, Parkville, Victoria 3010, Australia

[3] Monash Institute of Pharmaceutical Sciences, 381 Royal Parade, Parkville, VIC 3052, Australia

[4]ARC Centre of Excellence in Convergent Bio-Nano Science and Technology, Monash University, Parkville, Australia

Supplemental Material

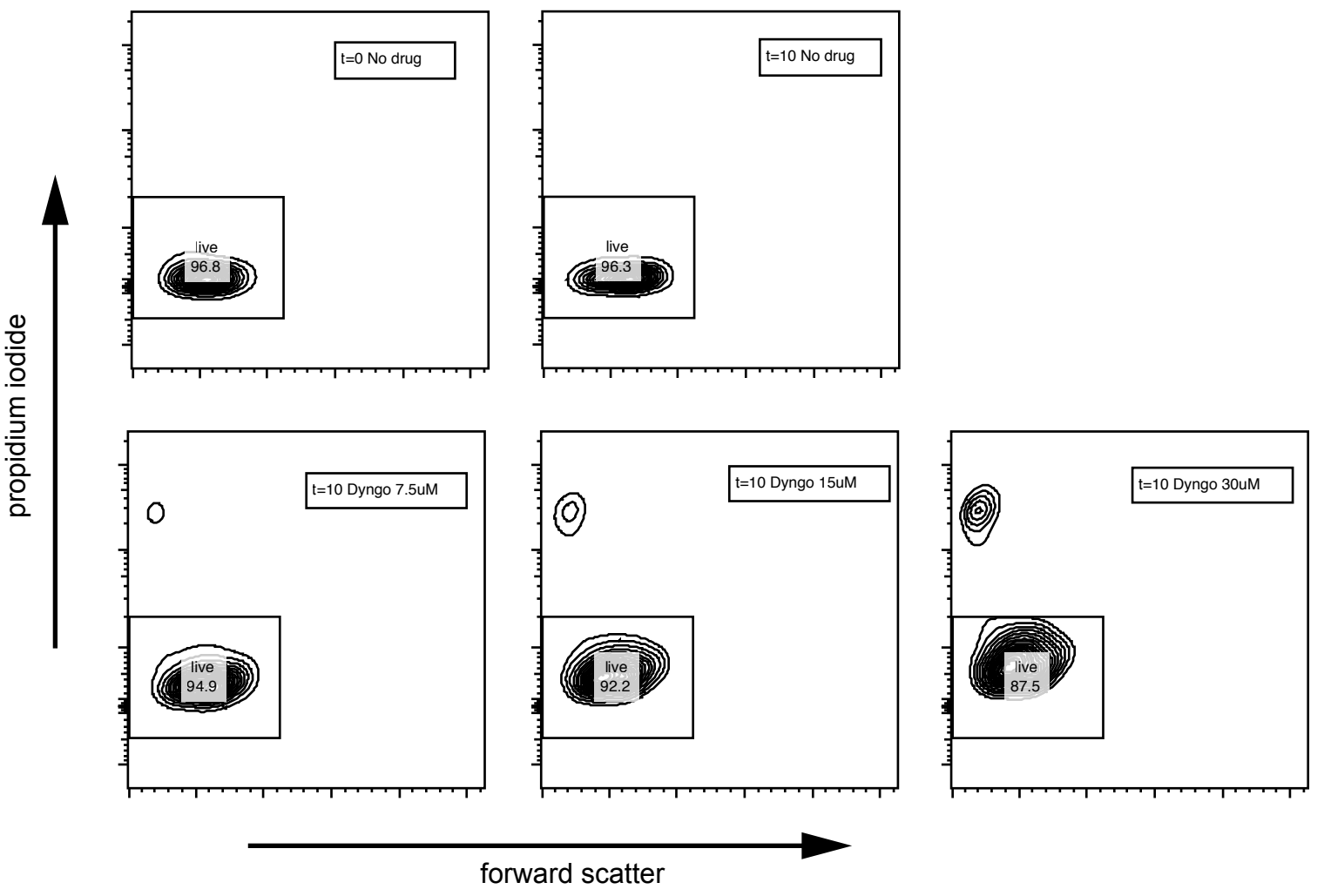

Figure S1. Cell viability in presence of Dyngo. C1R cells were incubated in the presence of increasing concentrations of Dyngo 4a for 45 minutes at 37°C. Cells were stained with the propridium iodide and viability assessed by flow cytometry.

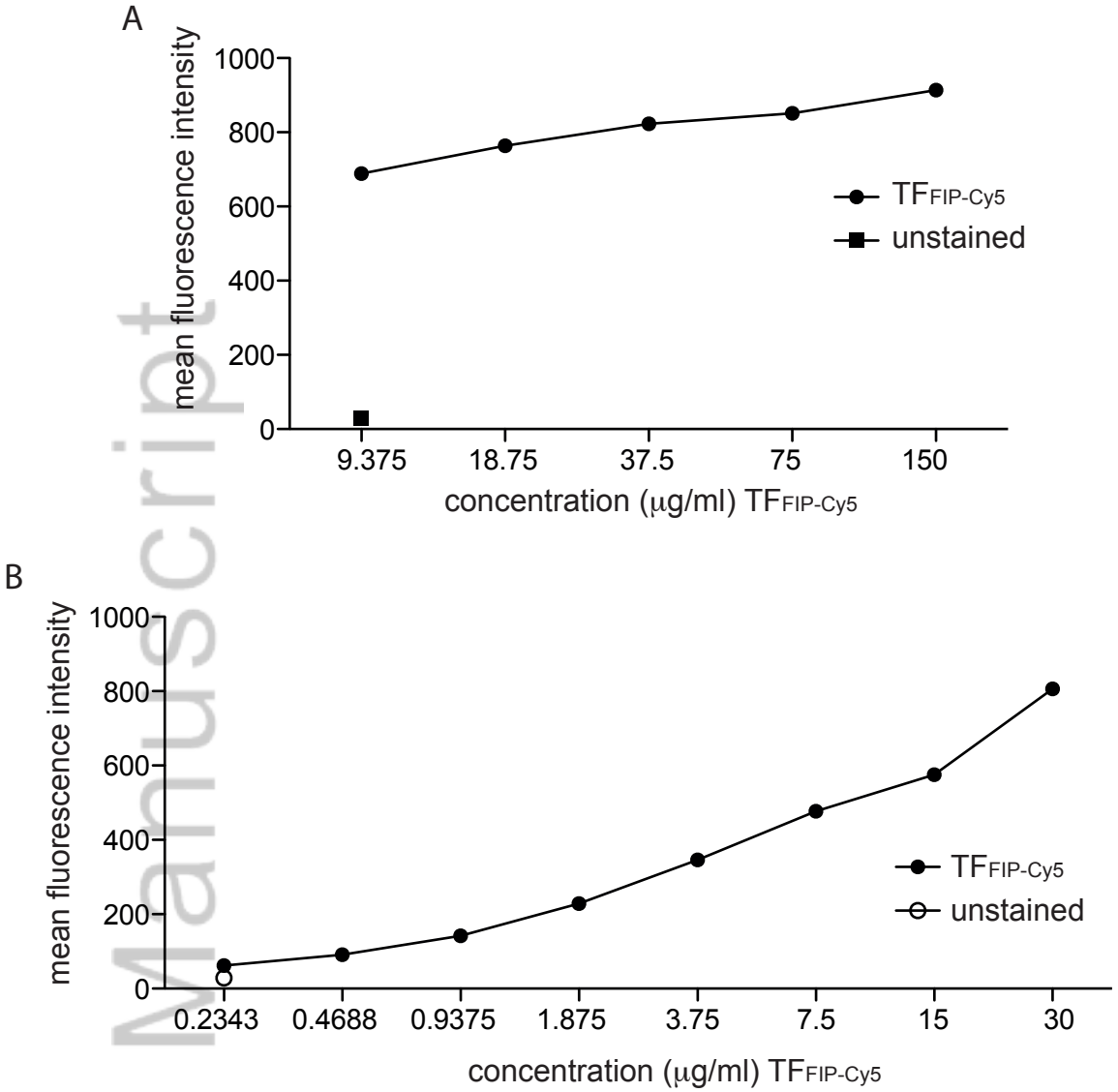

Figure S2. Titration of TF-FIP-Cy5. C1R cells were incubated with increasing concentrations of TF-FIP-Cy5 for 30 mins on ice. Excess TF-FIP-Cy5 was washed away and the cells were examined by flow cytometry. Panel A and B were performed as independent experiments.

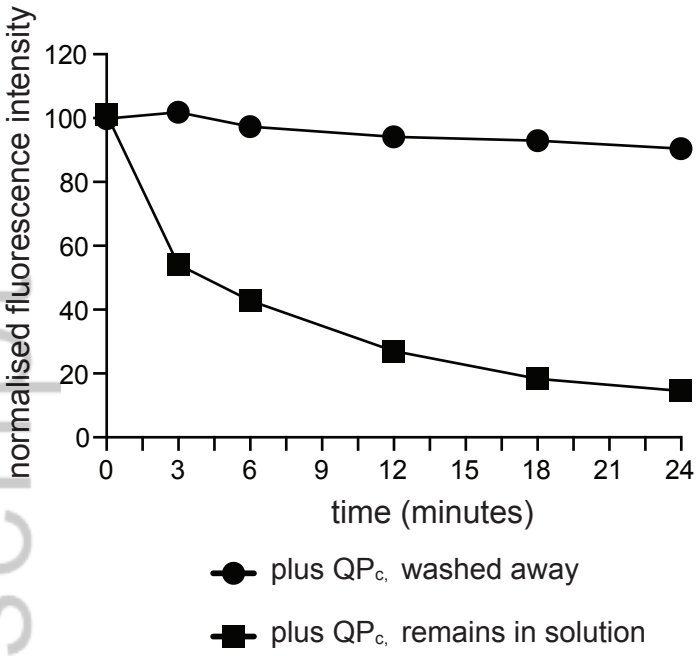

Figure S3. Internalization of QPc. C1R cells were labeled with anti-TFR-FIP at 4°C. After receptor binding, cells were incubated at 37ºC for for increasing periods of time before analysis with flow cytometry. Cells with internalised anti-TFR-FIP were incubated with QP_c and the proble left in the media (squares) or the cells were incubated with QP_c for 1 min, followed by 3 washes with PBS (circles). Fluorescence for all samples was normalized to 100% for the 0 time point immediately following addition of QP_c. The decline in fluorescence intensity in conditions where

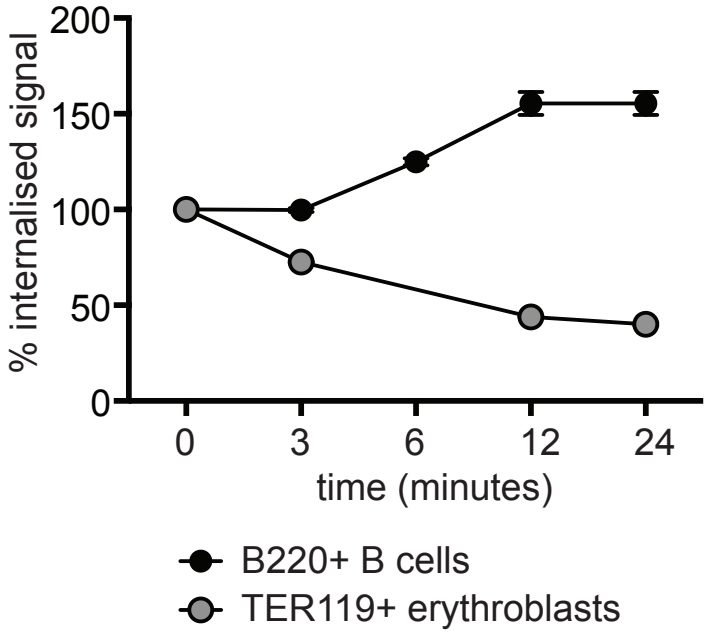

Figure S4. Change in fluorescence intensity after initial quenching. Bone marrow erythroblasts (red) and B220+ B cells (blue), were incubated with anti-TFR-FIP at 4°C. After receptor binding, cells were incubated at 37ºC for 6 min, cells were placed on ice and incubated with 1 μM QPc for 1 min. Excess QPc was washed away after the 1 min incubation. The cells were then incubated at 37°C for increasing periods of time, with the fluorescence intensity normalised to 100% at the start of the recycling period. The increase in fluorescence intensity of the B220 cells indicates the denaturation of the FIP QPc complex. The decrease in intensity for the bone marrow erythroblasts is indicative of loss of anti-TFR from the cell due to recycling.